7778 J. Med. Chem. 2009, 52, 7778–7787
DOI: 10.1021/jm900843g

Journal of Medicinal Chemistry Article

Inhibitors of Human Immunodeficiency Virus Type 1 (HIV-1) Attachment. 5. An Evolution from Indole to Azaindoles Leading to the Discovery of 1-(4-Benzoylpiperazin-1-yl)-2-(4,7-dimethoxy-1*H*-pyrrolo[2,3-*c*]-pyridin-3-yl)ethane-1,2-dione (BMS-488043), a Drug Candidate That Demonstrates Antiviral Activity in HIV-1-Infected Subjects[∞]

Tao Wang,*[,†] Zhiwei Yin,[†] Zhongxing Zhang,[†] John A. Bender,[†] Zhong Yang,[†] Graham Johnson,[†] Zheng Yang,[‡] Lisa M. Zadjura,[‡] Celia J. D'Arienzo,[‡] Dawn DiGiugno Parker,[§] Christophe Gesenberg,[§] Gregory A. Yamanaka,[∥,#] Yi-Fei Gong,[∥] Hsu-Tso Ho,[∥] Hua Fang,[∥] Nannan Zhou,[∥] Brian V. McAuliffe,[∥] Betsy J. Eggers,[∥] Li Fan,[∥] Beata Nowicka-Sans,[∥] Ira B. Dicker,[∥] Qi Gao,[⊥] Richard J. Colonno,[∥] Pin-Fang Lin,[∥] Nicholas A. Meanwell,[†] and John F. Kadow*[,†]

[†]*Departments of Chemistry and* [‡]*Metabolism and Pharmacokinetics, Preclinical Candidate Optimization and* [§]*Discovery Pharmaceutics and* [∥]*Virology, Bristol-Myers Squibb Research and Development, 5 Research Parkway, Wallingford, Connecticut 06492, and* [⊥]*Analytical Research and Development, Bristol-Myers Squibb Research and Development, 1 Squibb Drive, New Brunswick, New Jersey 08901.* [#] *Deceased June 27th, 2005.*

Received June 10, 2009

Azaindole derivatives derived from the screening lead 1-(4-benzoylpiperazin-1-yl)-2-(1*H*-indol-3-yl)ethane-1,2-dione (**1**) were prepared and characterized to assess their potential as inhibitors of HIV-1 attachment. Systematic replacement of each of the unfused carbon atoms in the phenyl ring of the indole moiety by a nitrogen atom provided four different azaindole derivatives that displayed a clear SAR for antiviral activity and all of which displayed marked improvements in pharmaceutical properties. Optimization of these azaindole leads resulted in the identification of two compounds that were advanced to clinical studies: (*R*)-1-(4-benzoyl-2-methylpiperazin-1-yl)-2-(4-methoxy-1*H*-pyrrolo[2,3-*b*]pyridin-3-yl)ethane-1,2-dione (BMS-377806, **3**) and 1-(4-benzoylpiperazin-1-yl)-2-(4,7-dimethoxy-1*H*-pyrrolo[2,3-*c*]pyridin-3-yl)ethane-1,2-dione (BMS-488043, **4**). In a preliminary clinical study, **4** administered as monotherapy for 8 days, reduced viremia in HIV-1-infected subjects, providing proof of concept for this mechanistic class.

Introduction

The human immunodeficiency virus (HIV) infection pandemic is now over 25 years old and continues to be a major medical threat to human kind.[1−4] By the end of 2005, 40 million people worldwide were estimated to be infected with HIV, and deaths from its sequelae, acquired immunodeficiency syndrome (AIDS[a]), were occurring at the rate of approximately 3 million people per annum. Highly active antiretroviral therapy (HAART) has helped to decelerate the spread of the HIV/AIDS epidemic in many parts of the world and has turned HIV into a chronic disease for many infected individuals. However, with long-term HAART, the development of resistance has emerged as a concern of considerable importance.[5−10] More than 70% of patients currently relying on antiretroviral therapy (ART) have developed some detectable level of resistance,[5] and 20% of new infections carry key mutations to existing drug classes.[9,10]Thus, there remains a need for the discovery and development of new anti-HIV agents with mechanisms that are distinct from the 31 currently marketed drugs, a pharmacopeia comprising 17 nucleoside and non-nucleoside reverse transcriptase inhibitors, 11 protease inhibitors, 1 integrase inhibitor, 1 fusion inhibitor, and 1 CCR5 coreceptor antagonist.[11] In principle, mechanistically novel inhibitors should not be cross-resistant to the existing anti-HIV/AIDS drugs and would find utility in drug combinations aimed at salvage or, eventually, first line therapy. An early and important event in HIV infection

[∞] We dedicate this article to the memory of Dr. Gregory Yamanaka, a valued and highly respected colleague who contributed significantly to antiviral drug discovery at Bristol-Myers Squibb. Greg was a biochemist involved in fundamental aspects of the biochemical profiling of two marketed antiviral drugs, the HIV protease inhibitor atazanavir, marketed as Reyataz, and the nucleoside-based HBV inhibitor entecavir, marketed as Baraclude.

*To whom correspondence should be addressed. For T.W.: phone, 203-677-6584; fax, 203-677-7702; e-mail, tao.wang@bms.com. For J.F.K.: phone, 203-677-6910; fax, 203-677-7702; e-mail, john.kadow@bms.com.

[a] Abbreviations: HIV-1, human immunodeficiency virus type 1; AIDS, acquired immunodeficiency syndrome; HAART, highly active antiretroviral therapy; ART, antiretroviral therapy; gp120, glycoprotein 120; CCR5, chemokine (C−C motif) receptor 5; CXCR4, chemokine (C−X−C motif) receptor 4; CD4, cluster of differentiation 4; IC_{50}, 50% inhibitory concentration; EC_{50}, 50% effective concentration; CC_{50}, 50% cytotoxic concentration; DMEM, Dulbecco's modified Eagle medium; FBS, fetal bovine serum; Luc, luciferase; LTR, long terminal repeat; XTT, 2,3-bis(2-methoxy-4-nitro-5-sulfophenyl)-2*H*-tetrazolium-5-carboxanilide inner salt; PBMC, peripheral blood mononuclear cells; HeLa cells, Henrietta Lacks cell line; CYP 450, cytochrome P450; QT interval, a measure of the time between the start of the Q wave and the end of the T wave in the heart's electrical cycle; hERG, the human ether-a-go-go related gene; Caco cells, human colorectal adenocarcinoma cells; HLM, human liver microsomes; SAR, structure−activity relationship; $T_{1/2}$, half-life; AUC, area under the curve; C_{max}, the maximum concentration of a drug in the body after dosing; C_{min}, the minimum concentration that a drug achieves in a tested area after the drug has been administrated and prior to the administration of a second dose; LC, liquid chromatography; HPLC, high pressure liquid chromatography; MS, mass spectrometry; HRMS, high resolution mass spectrometry; DEBPT, 3-(diethoxyphosphoryloxy)-1,2,3-benzotriazin-4(3*H*)-one; PEG, poly(ethylene glycol); Bz, benzoyl; MeOH, methanol; EtOH, ethanol; Et_3N, triethylamine; THF, tetrahydrofuran; EtOAc, ethyl acetate; $MgSO_4$, magnesium sulfate; K_2CO_3, potassium carbonate; Na_2CO_3, sodium carbonate; $AlCl_3$, aluminum chloride; NH_4Cl, ammonium chloride; DMSO, dimethyl sulfoxide; NaOMe, sodium methoxide; KOMe, potassium methoxide; CuI, copper(I) iodide; CH_2Cl_2, methylene chloride; $NaHCO_3$, sodium bicarbonate; HCl, hydrogen chloride; DMF, *N*,*N*-dimethylformamide; $^iPr_2NEt$, diisopropylethylamine.

 Published on Web 09/21/2009

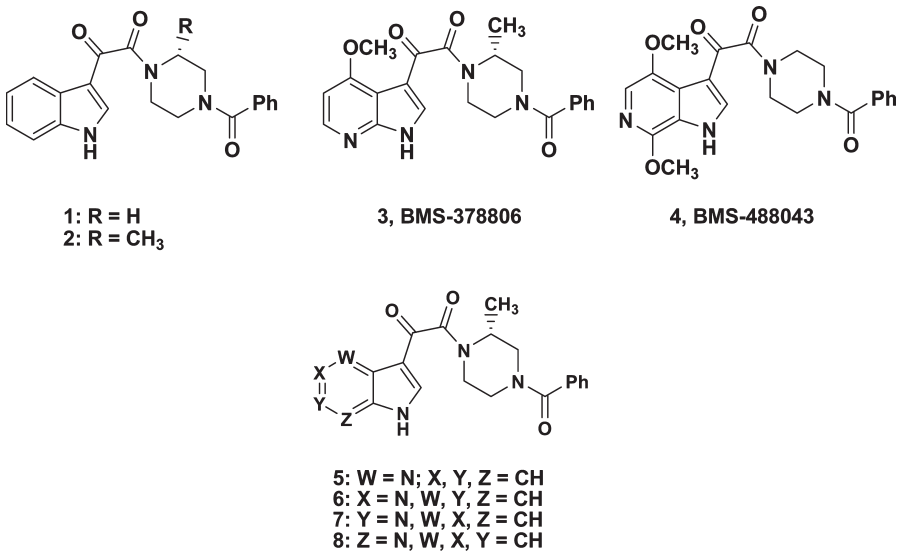

Figure 1. HIV-1 attachment inhibitors.

involves the formation of a specific interaction between the membrane-bound HIV-1 glycoprotein 120 (gp120) and CD4, a host cell protein expressed on human T cells and macrophages that is the primary receptor for HIV-1.[12] The interaction of HIV-1 with CD4 is an essential prelude to subsequent biochemical steps that are necessary for efficient HIV-1 entry into the host cell cytosol where the process of replication can be initiated. An interruption of the interaction of viral gp120 with CD4 would be expected to interfere with HIV-1 infectivity at a very early step of the viral life cycle, a potentially attractive target for systemic therapy and topical (microbicidal) prophylaxis.[13−24] We have pioneered a series of small molecules that interfere with the interaction between HIV-1 gp120 and the host cell receptor and have described progress toward identifying inhibitors that meet target criteria for clinical evaluation.[25−32]Preliminary mechanistic studies indicate that this class of HIV-1 attachment inhibitor binds to viral gp120 and stabilizes a conformation not recognized by CD4.[28−30] However, under different experimental conditions, compounds of this class may form a ternary complex with gp120 and CD4 and interfere with CD4-induced exposure of the HIV gp41 heptad repeats, the assembly of which is a critical event in virus-host cell membrane fusion.[31,32] Optimization of a screening lead, the indoleglyoxamide derivative **1** (Figure 1) which was identified using a cell-based assay, provided potent inhibitors of HIV-1 infection in vitro.[26,27] However, additional preclinical profiling of **1** and its close analogues surfaced limitations associated with the physicochemical properties of this class of HIV-1 inhibitor that compromised efficient drug formulation and delivery. In an effort to address this problem, which was attributed in part to the properties inherent to the indole heterocycle, we prepared the four possible unsubstituted azaindole analogues of indole **2** (Figure 1), used as the prototype for this study, and compared their in vitro profiles. In this article, we describe the results of this survey and the subsequent chemical optimization that led to the identification of two compounds that were advanced to clinical studies: the 7-azaindole HIV-1 attachment inhibitor BMS-378806 (**3**)[26,28]and the 6-azaindole derivative BMS-488043 (**4**).[30] Clinical studies with **4** have validated HIV-1 attachment inhibition as a potential approach to the control of HIV-1 infection in vivo.[33]

Results and Discussion

The indole **2** inhibited virus entry in a pseudotype assay using envelopes from the CCR5-dependent JRFL strain and CXCR4-dependent LAI strain of HIV-1 with EC_{50} values of 4.0 and 4.9 nM, respectively, and was not overtly cytotoxic to the HeLa host cell line (Table 1). In order to provide benchmark data for the series, this compound was profiled extensively in a series of in vitro assays designed to predict aspects of the clinical performance of the molecule and identify potential problems that would interfere with preclinical and/or clinical development. When incubated in a human liver microsomal preparation, the half-life for the disappearance of **2** was 16.9 min, an interval considered to predict an intermediate clearance rate in humans based on comparison to standards. However, compound **2** had the potential to be well absorbed in vivo based on its high permeability across a layer Caco-2 cells grown to confluence (P_c = 169 nm/s at pH 6.5). The compound inhibited three CYP 450 enzymes considered to be of clinical importance, with IC_{50} values of 2.6, 5.2, and 4.8 μM toward the 2C19, 2C9, and 2D6 isoforms, respectively. Although this inhibition was of modest potency, the data were sufficient to provoke some concern for the potential for drug−drug interactions in vivo and assessment of this aspect of the biochemical pharmacology was incorporated into the screening paradigm. Indole **2** was predicted to have low potential for cardiac toxicity due to the induction of QT rhythm abnormalities related to inhibition of the rapid component of the delayed rectifier cardiac K^+ channel encoded by the hERG gene based on an IC_{50} value of >80 μM in a channel flux assay. However, the solubility of a crystalline form of **2** in an aqueous buffer solution at pH 6.5 was low (16 μg/mL) and the molecule offered limited potential for formulation as a salt because of the absence of basic functionality and the high pK_a of the indole NH. Collectively, these data identified several weaknesses in the profile of **2** that became the focus of an optimization campaign, most notably the modest stability in HLM and the low aqueous solubility.

To assess the potential for addressing liabilities associated with the indole chemotype, modification of the phenyl ring of the core heterocycle was examined in the context of the four possible azaindole isomers **5**−**8** (Figure 1), which were

Table 1. Comparison of the HIV-1 Inhibitory Activity, in Vitro Profiling, and Physicochemical Properties of HIV-1 Attachment Inhibitors

compd	antiviral EC_{50} (nM)	cytotoxicity (MT-2 cells) CC_{50v} (μM)	stability in human liver microsomes (HLM) $T_{1/2}$ (min)	inhibition of CYP 450 enzymes IC_{50} (μM)[a]	hERG IC_{50} (μM)	Caco-2 permeability P_c at pH 6.5 (nm/s)	crystalline solubility at 25 °C and pH 6.5 (mg/mL)	pK_a	log D at pH 6.5	mp (°C)	specific optical rotation (deg g^{-1} mL^{-1} dm^{-1})
2	4.0 (2.4, 5.7) (JRFL) 4.9 (7.7, 2.0) (LAI)	200 (237, 153)	16.9	1A2: > 40 2C19: 2.6 2C9: 5.2 2D6: 4.8 3A4-1: > 40 3A4-2: > 40	> 80	169	0.016	10.9	1.9	212−216	$[\alpha]^{20}_D = -7.18$
5	1.6 (1.7, 1.5) (JRFL)	> 300 (n = 2)	> 100	1A2: > 40 2C19: 36 2C9: > 40 2D6: > 40 3A4−1: > 40 3A4-2: > 40	> 80	76	0.932	5.0, 9.8	0.9	298−301	$[\alpha]^{20}_D = -19.88$
6	575.9 (514.2, 637.6) (JRFL)	> 300 (n = 2)	> 100	1A2: > 40 2C19: 17 2C9: > 40 2D6: > 40 3A4-1: 18 3A4-2: 9.3	> 80	19	0.419	6.2, 9.8	1.2	227	$[\alpha]^{20}_D = -3.39$
7	21.6 (9.5, 33.6) (JRFL)	> 300 (n = 2)	38.5	1A2: > 40 2C19: 7.2 2C9: 17 2D6: 38 3A4-1: > 40 3A4-2: > 40	> 80	< 15	0.487	6.0, 9.3	1.5	249−253	$[\alpha]^{20}_D = -5.15$
8	1.7 ± 1.6 (n = 11) (JRFL)	280 (296, 265)	49.5	1A2: > 40 2C19: 10 2C9: 7.9 2D6:17 3A4-1: > 40 3A4-2: > 40	> 80	168	0.936	2.0, 9.7	1.8	146−148	$[\alpha]^{20}_D = -6.28$
3	1.47 ± 0.63 (JRFL) 2.68 ± 1.64 (LAI)	> 300	37	1A2: > 40 2C19: > 40 2C9: > 40 2D6: 9.7 3A4-1: > 40 3A4-2: > 40	> 80	51	~0.2 1.3 at pH 2.1 3.3 at pH 11	2.9, 9.6	1.6	236	$[\alpha]^{23}_D = -5.14$
4	0.88 ± 0.46 (n = 56) (JRFL) 1.15 (1.15, 1.15) (LAI)	> 300	> 100	1A2: > 40 2C19: > 40 2C9: 30 2D6: > 40 3A4-1: > 40 3A4-2: > 40	> 80	178	~0.04 0.9 at pH 1.5 0.25 at pH 10	2.9, 9.3	1.5	229.5−232	

[a] Substrates used for CYP 450 inhibition studies: 1A2 and 2C19, 3-cyano-7-ethoxycoumarin; 2C9, 7-methoxy(trifluoromethyl)coumarin; 2D6, 3-[2-(*N*,*N*-diethyl-*N*-methylammonium)ethyl]-7-methoxy-4-methylcoumarin; 3A4-1, benzyloxy-4-(trifluoromethyl)coumarin; 3A4-2, 7-benzyloxyresorufin.

evaluated in a pseudotype assay using the CCR5-dependent JRFL HIV-1 strain envelope. As illustrated in Table 1, the introduction of a nitrogen atom resulted in molecules with substantially different in vitro profiles when compared to the parent molecule **2**. The HIV-1 inhibitory activity of **2** was fully preserved with the 4-aza isomer **5** and the 7-aza isomer **8**, EC_{50} values of 1.6 and 1.7 nM, respectively. However, when the nitrogen atom was incorporated at a more exposed position of the core, antiviral potency was reduced, with the 6-aza isomer **7** a modest 5-fold less potent than **2**, EC_{50} = 22 nM, and the 5-aza analogue **6** a more dramatic 100-fold weaker, EC_{50} = 576 nM. However, the azaindole series demonstrated uniformly improved profiles in assays predictive of pharmacokinetic and pharmaceutical performance. The half-life in human liver microsomes (HLM) for the four isomers varied from 38.5 to >100 min, representing a marked enhancement in metabolic stability compared to **2** that indicated reduced potential for first-pass metabolism in humans. This result may be related, in part, to the improved aqueous solubility determined for this family of azaindoles **5**−**8** at pH 6.5, which is at least 25-fold higher than that measured for the indole **2**. The basic nitrogen atom of the azaindole ring (pK_a = 2.0−6.2) offered additional avenues and options for formulation based on the potential for salt formation, although stronger acids would be required for the less basic isomers.[34] The increased basicity associated with the azaindole core appeared to correlate with the permeability of these compounds across a Caco-2 monolayer at pH 6.5. The highly permeable 7-azaindole **8** (pK_a = 2.0) would be expected to exist almost exclusively as the free base at pH 6.5 while a small fraction of the 4-azaindole **5** (pK_a = 5.0) would be present as the pyridinium cation, leading to reduced permeability. In contrast, a considerable amount of both the 5-azaindole **6**, pK_a = 6.2, and 6-azaindole **7**, pK_a = 6.0, would exist in the protonated form at pH 6.5, which would reduce the rate of permeation across the Caco-2 membrane. However, it was anticipated that the basicity of the azaindoles could be modulated by the judicious deployment of substituents (vide infre). Altering the core heterocycle did not introduce any additional safety liabilities based on the in vitro profiling data which included assessments that predict cytotoxicity, hepatotoxicity, and cardiotoxicity. Of some concern with the incorporation of pyridine-like structural elements was the potential for increased CYP 450 inhibition.[35,36] However, although signals were observed within the matrix of compounds and recombinant enzymes tested, there were no clear and consistent trends and all four azaindole isomers appeared to offer some improvement over the parent compound **2**.

The in vitro profile of the 7-azaindole **8** was encouraging, and optimization of this chemotype was facilitated by the commercial availability of the parent heterocycle. This initiative took advantage of early structure−activity relationships (SARs) developed for the indole series and resulted in the identification of the 4-methoxy-7-azaindole derivative **3**, the first HIV attachment inhibitor to enter clinical studies designed to validate this mechanistic approach to the control of HIV-1.[26] Unfortunately, **3** failed to achieve targeted plasma concentrations following oral administration to humans, an outcome attributed to a combination of moderate stability in HLM, $T_{1/2}$ = 37 min, and Caco-2 cell permeability (P_c = 51 nm/s) at the lower end of the range that would predict good intestinal absorption in humans.[33]

In an effort to identify compounds with improved potency, attention was focused on the 6-azaindole series represented by **7**, since this isomer uniquely combined good intrinsic potency with an opportunity to simultaneously substitute at C-4 and C-7, a pattern associated with improved antiviral activity in the indole series.[27] Of particular interest in this context, the introduction of a methoxy substituent at C-7 was anticipated to not only enhance antiviral activity but also reduce the basicity of the azaindole nitrogen atom, thereby leading to enhanced membrane permeability.[37,38] The substantial electron withdrawing properties of a methoxy substituent adjacent to the N atom of pyridine are clearly reflected in the increased acidity of the conjugate acid of 2-methoxypyridine, pK_a = 3.06, compared to protonated pyridine, which has pK_a = 5.23.[37,38] This is attributed to an electronegative effect mediated through the C−O σ-bond that depends on proximity. In contrast, a 4-methoxy substituent increases the basicity of pyridine (pK_a = 6.47), the result of the dominance of electron donation via resonance through the π system. The reduced basicity of the 6-aza nitrogen atom combined with steric shielding by the methoxy substituent would also be expected to attenuate the potential for oxidative metabolism to the *N*-oxide and help to mitigate the potential for inhibition of CYP 450 enzymes.[35,36] To further improve the metabolic stability in HLM, the methyl subsituent attached to the piperazine ring that was introduced with **3** was omitted, since SAR from a related series suggested that this group is susceptible to metabolic modification. The key challenge was to identify a molecule with the correct balance of potency and metabolic stability that did not sacrifice solubility and membrane permeability, an analysis that rationalized the 4,7-dimethoxy-6-azaindole derivative **4** as a target molecule.

The 6-azaindole **4** was initially prepared from commercially available 5-bromo-2-chloro-3-nitropyridine (**9**), as described in Scheme 1. Treating **9** with 3−4 equiv of vinylmagnesium bromide at −78 to −20 °C afforded 4-bromo-7-chloro-6-azaindole (**10**) in yields of up to 35%.[39] A copper-catalyzed tandem displacement of the chlorine and bromine atoms by NaOMe or KOMe provided 4,7-dimethoxy-6-azaindole (**11**) in yields as a high as 75%.[40,41] A Friedel−Crafts type reaction of **11** with either methyl or ethyl chlorooxoacetate promoted by an excess of $AlCl_3$[42] generated an ester **12** which was hydrolyzed to the acid salt **13** using K_2CO_3 in aqueous MeOH. In the final step, the acid salt **13** was coupled with *N*-benzoylpiperazine using 3-(diethoxyphosphoryloxy)-1,2,3-benzotriazin-4(3*H*)-one (DEBPT)[43] as the dehydrating agent to afford **4** in an overall isolated yield of up to 37% from the azaindole **11**. The structure of **4** was confirmed by single crystal X-ray structure analysis and compared with that of **3** (Figure 2).[44] In the solid state the 2-keto moiety of both molecules is oriented away from 4-methoxy substituent of the azaindole ring, while the two carbonyl moieties are orthogonal to each other. In addition, both piperazine nitrogen atoms in each molecule are sp^2 hybridized, resulting in a planar arrangement of the proximal atoms while the phenyl group is distorted from coplanarity with the amide carbonyl as a function of allylic 1,3-strain.[45−47]In the solid state, the piperazine methyl group of **3** adopts an axial disposition to avoid unfavorable allylic 1,3-strain with the amide carbonyl oxygen atom.[45−48]

The in vitro profiling of **4** revealed a compound with physical properties (pK_a, log *D*, and melting point) that exhibited considerable similarity to those of **3**, as summarized in Table 1. However, notable differences between the two compounds are the enhanced Caco-2 cell permeability and

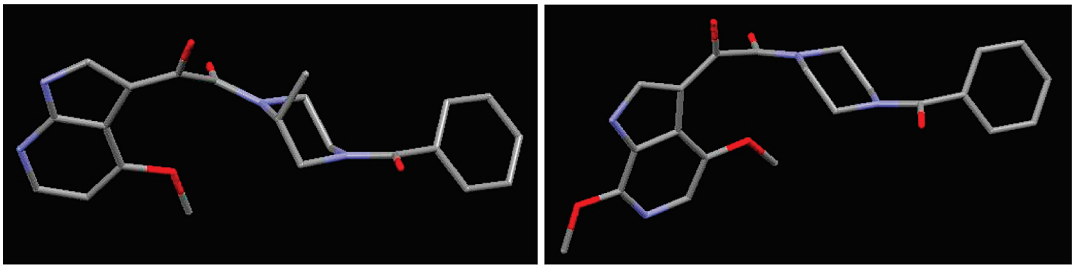

Figure 2. X-ray crystallographic structures of **3** and **4**.

Scheme 1. Discovery Synthesis of Compound **4**

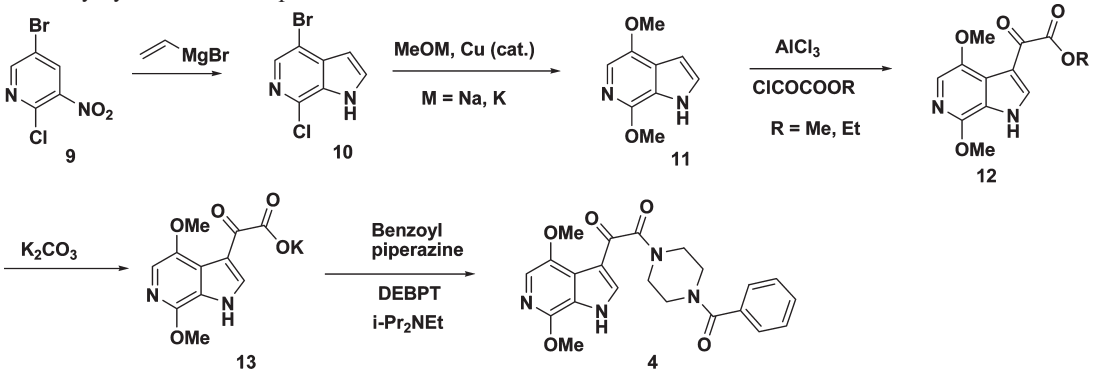

increased stability in HLM associated with **4**, positive attributes counterbalanced by a 5-fold reduction in solubility at pH 6.5, a difference that is, however, eroded at lower pH.

The antiviral properties of **4** compare favorably with those of **3** toward the laboratory strain of HIV-1 used for screening (Table 1). As is typical for this series of HIV-1 attachment inhibitor, viruses expressing a B-clade envelope protein are more susceptible than other clades and **4** displayed a median EC_{50} of 36.5 nM toward 40 clinical isolates, which compares to 61.5 nM for **3**.[49]

The pharmacokinetic properties of **4** were examined in detail in several preclinical species.[50] The oral bioavailability of **4** in rats, dogs, and monkeys following administration as a solution in 90% PEG400/10% EtOH was 90%, 57%, and 60%, respectively. This compares to an oral bioavailability of 19%, 77%, and 24%, respectively, for **3** in the same species and reflects the enhanced membrane permeability of **4** observed in Caco-2 cells and improved metabolic stability in rat, dog, and monkey liver microsomes.[50] Detailed comparative pharmacokinetic data for **3** and **4** in the rat are compiled in Table 2. The overall exposure of **4** as assessed by AUC was over 10-fold higher when compared to **3**, with a terminal intravenous half-life 8-fold longer and a C_{max} 20-fold higher. Total body clearance was low in rats, dogs, and monkeys, predicted effectively by in vitro liver microsomal stability data, with the result that plasma levels at 12 h after oral dosing were 18- to 160-fold higher than the median antiviral EC_{50} toward the panel of 25 clinical isolates. Clearance in humans was predicted to be low (1.5−3.0 (mL/min)/kg) based on human liver microsomal stability data or allometric scaling of the animal pharmacokinetic profiles, with the latter predicting a half-life in humans of over 3 h.[50] The oral bioavailability of **4** after administering a crystalline suspension (mean particle size of ~7 μm) to rats at a dose of 5 mg/kg was 55%, indicative of reasonable dissolution in gastrointestinal fluid. Collectively, these profiling data predicted that **4** should have improved oral exposure in humans compared to BMS-378806 (**3**), with the potential for boosting by coadministration of the CYP 3A4 inhibitor ritonavir, since **4** is primarily metabolized by this enzyme in vitro.[50] Azaindole **4** was, however, considered unlikely to be a perpetrator of drug−drug interactions based on its lack of significant inhibitory activity toward a panel of recombinant CYP 450 enzymes, $IC_{50} > 30$ μM.

Table 2. Pharmacokinetic Profile of Compounds **3** and **4** in the Rat

	compound	
parameter	**3**	**4**
dose (mpk)	5	5
oral C_{max} (μg/mL)	0.09	1.9
oral AUC ((μg/h)/mL)	0.5	6.3
iv terminal $T_{1/2}$ (h)	0.3	2.4
bioavailability (%)	19	90

The 6-azaindole **4** is a crystalline, nonhygroscopic solid that melts at 229.5−232 °C and displays good stability as the solid, suffering no degradation for at least 4 weeks at temperatures up to 50 °C and 75% relative humidity at 40 °C. The compound is soluble at 0.9 mg/mL at pH 1.5 and 0.04 mg/mL at pH 4−8 and shows excellent stability in solution at pH 2 and pH 7 with no observed chemical changes observed after 48 h at 37 °C.

Azaindole **4** possessed a clean preclinical safety profile, showing no significant cytotoxicity toward 11 human cell lines that included T-cells, peripheral blood monocytes (PBMC), hepatocarcinoma, neuronal tumors, cervical, lung, and larynx carcinomas and embryonic kidney cells, $CC_{50} \geq 120$ μM. Similarly, the compound was not toxic to hepatocytes in vitro at concentrations up to 200 μM in the absence or presence of expression of any of the four major CYP 450 enzymes. The lack of detectable blockade of the hERG rapid delayed rectifier K^+ ion channel at concentrations of 80 μM in vitro (Table 1) was confirmed in vivo with no drug-related ECG changes observed in dogs at doses as high as 200 mpk, which afforded $C_{max} = 33$ μM. In exploratory toxicology studies, **4** was well tolerated when given orally to rats for 2 weeks at daily

doses of up to 200 mg/kg and to dogs for 10 days at daily doses of up to 100 mg/kg, with the C_{min} being 58- and 160-fold the median EC_{50} at the higher doses, respectively. Additionally, **4** was not mutagenic in an Ames reverse-mutation assay at concentrations of up to 5 mg/plate and the compound exerted no significant effects toward a panel of 53 in vitro biochemical assays at 10 μM. These data revealed a safety profile consistent with exploring **4** in phase 1 clinical studies in normal healthy volunteers and proof-of-concept studies in HIV-1-infected subjects.[33]

Pharmacokinetic studies in normal healthy volunteers under fasting conditions revealed that C_{max} and AUC increased in a dose-related but not dose-proportional fashion following administration of 200, 400, or 800 mg of **4** formulated in capsules.[51] Higher doses of 1200, 1800, or 2400 mg resulted in no significant increase in exposure. A solution dose of 200 mg resulted in a 3-fold increase in exposure of **4** compared to the tablet formulation, while pretreatment with ritonavir increased exposure by 43% at a dose of 400 mg and administration with food resulted in a 3- to 5-fold increase in exposure, higher following a high fat meal compared to a light meal, over a 400−1200 mg dose range.[51] In a multiple-dose study conducted in HIV-1-infected adults, the antiviral activity, safety, and tolerability of **4** were evaluated at doses of 800 or 1800 mg of drug administered with a high fat meal.[33] Patients received doses of either **4** or placebo every 12 h for 8 days, with no serious adverse events during the study. While none of the placebo-treated subjects had a maximal viral load decline of > 0.5 $\log_{10}$ copies/mL, 58% ($^7/_{12}$) of the patients treated with 800 mg of **4** had a viral load decline of > 1.0 $\log_{10}$ measured on day 8.[33] The results of this preliminary clinical study with **4** demonstrate that an orally bioavailable, small molecule HIV-1 attachment inhibitor can have potent antiviral activity in infected subjects.

Conclusions

In summary, an initial comparative survey demonstrated that azaindoles had the potential to address several of the key issues identified with indole-based HIV-1 attachment inhibitors, particularly low aqueous solubility and poor metabolic stability. Insights derived from the SAR associated with indole-based inhibitors anticipated the 4,7-dimethoxy-6-azaindole derivative **4**. This HIV-1 attachment inhibitor offered improved in vivo pharmacokinetic profiles in three species and appeared to address the low permeability and limited metabolic stability that were the most serious liabilities of **3**, a prototypical compound that showed insufficient exposure in human clinical studies.[33] The 6-azaindole **4** has established proof-of-concept for this mechanistically novel class of HIV-1 inhibitor in infected human subjects. However, despite the improvements described above, the pharmaceutical properties of **4** remain less than ideal. Oral dosing in conjunction with a high fat meal is required to provide targeted exposure in humans, an observation that prompted an exploration of additional formulation approaches designed to improve drug dissolution in the gastrointestinal tract.[44,52] An alternative solution to formulation and drug dissolution issues in the form of a prodrug will be described in future publications.[53]

Experimental Section

General Directions. ^{1}H and ^{13}C NMR spectra were obtained on a Bruker 500 Ultrashield NMR spectrometer operating at 500 MHz for ^{1}H and 125 MHz for ^{13}C.

All liquid chromatography (LC) data were recorded on a Shimadzu LC-10AS liquid chromotograph using a SPD-10AV UV−vis detector, and mass spectrometry (MS) data were determined with a Micromass Platform for LC operating in electrospray mode. The column used was selected from one of three: column A is a YMC ODS-A S7 3.0 mm × 50 mm column; column B is a PHX-LUNA C18 4.6 mm × 30 mm column; column C is an Xterra 4.6 mm × 50 mm C18 5 μm column. Gradient was performed from 100% solvent A/0% solvent B to 0% solvent A/100% solvent B (solvent A was 10% MeOH/90% H_2O/0.1% CF_3CO_2H; solvent B was 10% H_2O/90% MeOH/0.1% CF_3CO_2H). The flow rate was 5 mL/min, and the gradient time was 2 min with a holding time of 1 min. The detector wavelength was 220 nm.

Preparative HPLC methods were used to purify target compounds. Compounds purified by preparative HPLC were diluted in MeOH (1.2 mL) and purified on a Shimadzu LC-10A automated preparative HPLC system using the following methods: The column used was a YMC C18 S5 20 mm × 100 mm column with a detector operating at a wavelength of 220 nm. Purification ramped from the initial gradient (30% B, 70% A) to the final gradient (100% B, 0% A) over 20 min with holding for 3 min (100% B, 0% A). Solvent A was 10% MeOH/90% H_2O/0.1% CF_3CO_2H, and solvent B was 10% H_2O/90% MeOH/0.1% CF_3CO_2H.

Solubilities were measured 24−72 h after samples were added into phosphate buffered solution (pH 6.5) at room temperature. pK_a values were obtained via spectrophotometric titration method by using a pION GLpKa instrument. The log *D* values were determined using a classical octanol/water shake flask method using phosphate buffered solution at pH 6.5.

Melting points were determined using a TA SC 2920 modulated differential scanning calorimeter or EZ-Melt automated melting point apparatus.

Optical rotation values [α_D] were determined on solutions of the indole **2** and azaindoles **5**−**8** in MeOH−$CHCl_3$ (1:1) at a wavelength of 589 nm at 20 °C or a solution in MeOH for compound **3** at 23 °C.

The experimental methodology used to profile the Caco-2 permeability and liver microsomal stability of compounds **2**−**8** followed protocols previously described.[56]

(*R*)-1-(4-Benzoyl-2-methylpiperazin-1-yl)-2-(1*H*-pyrrolo[2,3-*b*]pyridin-3-yl)ethane-1,2-dione (**8**) and its precursors were prepared as previously reported.[26] The synthetic intermediates methyl 2-oxo-2-(1*H*-pyrrolo[3,2-*b*]pyridin-3-yl)acetate, methyl 2-oxo-2-(1*H*-pyrrolo[3,2-*c*]pyridin-3-yl)acetate, and methyl 2-oxo-2-(1*H*-pyrrolo[2,3-*c*]pyridin-3-yl)acetate were prepared as previously described.[42]

(*R*)-1-(4-Benzoyl-2-methylpiperazin-1-yl)-2-(1*H*-indol-3-yl)-ethane-1,2-dione (2). Et_3N (2 mL) was added to a solution of (*R*)-2-methyl-*N*-benzoylpiperazine (0.7 g, 3.43 mmol) and 2-(1*H*-indol-3-yl)-2-oxoacetyl chloride (0.5 g, 2.41 mmol) in dry THF. The mixture was stirred at room temperature for 16 h before being quenched by adding 10% brine solution (100 mL). The aqueous layer was extracted with EtOAc (2 × 100 mL) and the combined organic layers were dried over $MgSO_4$ and concentrated to give a residue, a portion of which (100 mg) was purified by preparative HPLC to afford **2**. HPLC retention time: 1.47 min (column C). Mp: 212−216 °C. $[\alpha]^{20}_D$ −7.18° (*c* 4.15 mg/mL). ^{1}H NMR (DMSO-d_6): δ 1.18 (b, 3H), 2.70−4.90 (m, 7H), 7.26−7.55 (m, 8H), 8.12−8.22 (m, 2H). ^{13}C NMR (DMSO-d_6): δ 14.6, 15.6, 44.0, 49.6, 58.8, 112.6, 113.0, 120.9, 122.5, 123.5, 124.8, 126.9, 128.4, 129.5, 135.4, 136.8, 136.9, 166.8, 170.1, 186.6. MS *m*/*z* $(MH)^+$ calcd for $C_{22}H_{22}N_3O_3$: 376.17; found 376.10. HRMS *m*/*z* $(MH)^+$ calcd for $C_{22}H_{22}N_3O_3$: 376.1661; found 376.1673. Anal. Calcd for $C_{22}H_{21}N_3O_3$: C, 70.38; H, 5.64; N, 11.19. Found: C, 69.99; H, 5.54; N, 10.99.

(*R*)-1-(4-Benzoyl-2-methylpiperazin-1-yl)-2-(1*H*-pyrrolo[3,2-*b*]-pyridin-3-yl)ethane-1,2-dione (5). Methyl 2-oxo-2-(1*H*-pyrrolo[3,

2-*b*]pyridin-3-yl)acetate (160 mg, 0.78 mmol) and K_2CO_3 (216 mg, 1.56 mmol) were dissolved in a 1:1 mixture of MeOH and H_2O (10 mL). After 16 h, LCMS analysis revealed 2-oxo-2-(1*H*-pyrrolo[3,2-*b*]-pyridin-3-yl)acetic acid (MS *m*/*z* calcd for $C_9H_7N_2O_3$ 191.05; found 190.87; HPLC retention time, 0.19 min (column A)) as the major product. A sample of 1 N HCl was added to the reaction mixture to adjust the pH to 5, the solvent removed under vacuum, and the residue dissolved in DMF (4 mL). (*R*)-2-Methyl-*N*-benzoylpiperazine·HCl (190 mg, 0.79 mmol), DEPBT (233 mg, 0.78 mmol), and ^{i}Pr$_2$NEt (0.4 mL) were added to the solution. The mixture was stirred at room temperature for 24 h, the solvents were removed in vacuo, and the residue was partitioned between 10% Na_2CO_3 and EtOAc. The organic layer was separated, dried over $MgSO_4$, and concentrated under vacuum and the residue purified by HPLC to afford **5** (13.2 mg, 4.5%). HPLC retention time: 0.96 min (column A). Mp: 298−301 °C. $[\alpha]^{20}_D$ −19.88° g^{-1} mL^{-1} dm^{-1} (*c* 3.77 mg/mL). ^{1}H NMR (CD_3OD−$CDCl_3$): δ 1.31 (b, 3H), 5.10−3.00 (m, 7H), 7.28 (m, 1H), 7.44 (s, 5H), 7.87 (m, 1H), 8.27 (d, 1H, J = 10.5 Hz), 8.56 (m, 1H). ^{13}C NMR (CD_3OD−$CDCl_3$): δ 14.7, 16.1, 45.5, 50.6, 113.2, 119.1, 121.5, 127.2, 129.0, 130.6, 131.0, 135.2, 138.2, 143.0, 145.2, 167.0, 172.4, 185.6. MS *m*/*z* (MH^+) calcd for $C_{21}H_{21}N_4O_3$: 377.16; found 377.14. HRMS *m*/*z* $(MH)^+$ calcd for $C_{21}H_{21}N_4O_3$: 377.1614; found 377.1625. Anal. Calcd for $C_{21}H_{20}N_4O_3\cdot0.4H_2O$: C, 65.75; H, 5.47; N, 14.60. Found: C, 65.52; H, 5.07; N, 14.49.

(*R*)-1-(4-Benzoyl-2-methylpiperazin-1-yl)-2-(1*H*-pyrrolo[3,2-*c*]-pyridin-3-yl)ethane-1,2-dione (6). Compound **6** was prepared from methyl 2-oxo-2-(1*H*-pyrrolo[3,2-*c*]pyridin-3-yl)acetate by following the general procedure described for **5** to afford 12.5 mg of product (4.3%). HPLC retention time: 0.89 min (column A). Mp: 227 °C. $[\alpha]^{20}_D$ −3.39° g^{-1} mL^{-1} dm^{-1} (*c* 3.85 mg/mL). ^{1}H NMR (CD_3OD): δ 1.35 (b, 3H), 4.90−3.10 (m, 7H), 7.51 (b, 6H), 8.16 (d, 1H, J = 5.8 Hz), 8.61 (d, 1H, J = 4.5 Hz), 8.72 (m, 1H), 9.62 (b, 1H). ^{13}C NMR (CD_3OD): δ 14.6, 15.8, 45.8, 50.6, 108.5, 114.2, 122.6, 127.1, 128.9, 130.5, 135.2, 138.7, 141.9, 142.4, 143.6, 166.6, 172.6, 185.1. MS *m*/*z* $(MH)^+$ calcd for $C_{21}H_{21}N_4O_3$: 377.16; found 377.15. HRMS *m*/*z* $(MH)^+$ calcd for $C_{21}H_{21}N_4O_3$: 377.1614; found 377.1630. Anal. Calcd for $C_{21}H_{20}N_4O_3$: C, 67.00; H, 5.35; N, 14.88. Found: C, 66.69; H, 5.21; N, 14.60.

(*R*)-1-(4-Benzoyl-2-methylpiperazin-1-yl)-2-(1*H*-pyrrolo[2,3-*c*]-pyridin-3-yl)ethane-1,2-dione (7). Compound **7** was prepared from methyl 2-oxo-2-(1*H*-pyrrolo[2,3-*c*]pyridin-3-yl)acetate following the procedure described for **5** to afford 12.7 mg of product (4.3%). HPLC retention time: 0.89 min (column A). Mp: 249−253 °C. $[\alpha]^{20}_D$ −5.15° g^{-1} mL^{-1} dm^{-1} (*c* 4.00 mg/mL). ^{1}H NMR (CD_3OD−$CDCl_3$): δ 1.28 (b, 3H), 5.10−3.10 (m, 7H), 7.46 (m, 5H), 8.34−8.18 (m, 3H), 8.81 (s, 1H). ^{13}C NMR (CD_3OD−$CDCl_3$): δ 14.5, 15.8, 45.7, 50.7, 113.8, 116.4, 127.1, 128.9, 130.4, 131.7, 134.8, 134.9, 135.3, 140.3, 140.9, 166.8, 185.8. MS *m*/*z* $(MH)^+$ calcd for $C_{21}H_{21}N_4O_3$: 377.16; found 377.10. HRMS *m*/*z* $(MH)^+$ calcd for $C_{21}H_{21}N_4O_3$: 377.1614; found 377.1632. Anal. Calcd for $C_{21}H_{20}N_4O_3\cdot0.3H_2O$: C, 66.06; H, 5.44; N, 14.67. Found: C, 65.94; H, 5.14; N, 14.46.

4-Bromo-7-chloro-1*H*-pyrrolo[2,3-*c*]pyridine (10). A solution of freshly prepared vinylmagnesium bromide in THF (3.92 L, 3.92 mol) was added via a cannula to a stirred solution of 5-bromo-2-chloro-3-nitropyridine (250 g, 1.05 mol) in THF (5 L) at −78 °C at such a rate that the temperature was maintained below −40 °C. The mixture was stirred for 1.5 h at −78 °C before being quenched with saturated aqueous NH_4Cl solution (1.5 L) and stirred for 16 h. The layers were separated. The aqueous layer was extracted with EtOAc (3 × 1 L) and the combined organic layer washed with brine and concentrated. The residue was dried under high vacuum and suspended in EtOAc (1 L) before being concentrated on a rotary evaporator (removed ∼800 mL of EtOAc) and cooled in a refrigerator for 1 h. The mixture was filtered and the collected solid washed with EtOAc (2 × 50 mL) and EtOAc/hexanes (1:1, 50, and 100 mL) before being dried under high vacuum to yield **10** (52.3 g, 22%) as a brown solid. LC purity: 95.7%. HPLC retention time: 1.62 min (column B). ^{1}H NMR (DMSO-d_6): δ 6.58 (s, 1H), 7.79 (s, 1H), 8.05 (s, 1H), 12.5 (br s, 1H). ^{13}C NMR (DMSO-d_6): δ 102.2, 110.9, 129.3, 131.6, 132.9, 134.4, 137.2. MS *m*/*z* $(MH)^+$ calcd for $C_7H_4BrClN_2$: 230.93; found 231.15.

4,7-Dimethoxy-1*H*-pyrrolo[2,3-*c*]pyridine (11). A three-neck, 3 L flask equipped with a Dean−Stark trap and an overhead stirrer was charged with MeOH (500 mL) and stirred under an atmosphere of N_2. KOMe (75.6 g, 1.08 mol) was added in portions followed by toluene (500 mL) and the solution stirred for 15 min until it became clear. Celite 545 (40 g), toluene (250 mL), 4,4-dibromo-7-chloro-1*H*-pyrrolo[2,3-*c*]pyridine (25.0 g, 108 mmol), and additional toluene (250 mL) were added, and the mixture was brought to reflux and held at 115 °C for 7 h while collecting a mixture of MeOH and toluene (600 mL total). The solution was cooled to ambient temperature, and LCMS analysis revealed 4-bromo-7-methoxy-1*H*-pyrrolo[2,3-*c*]pyridine (MS *m*/*z* $(MH)^+$ calcd for $C_8H_7BrN_2O$ 226.97; found 227.00. HPLC retention time of 1.20 min (column A)) as the major product. MeOH (500 mL) was added to the solution, and the temperature was once again increased to 115 °C. At 60 °C, CuI (22.6 g, 119 mmol) and MeOH (100 mL) were added and the mixture was held at 115 °C for 1.5 h while collecting a mixture of MeOH and toluene (750 mL total). The mixture was cooled to ambient temperature, and MeOH (500 mL) and NH_4Cl (58 g) were added. The solution was stirred for 1 h and concentrated to dryness. The residue was dissolved in EtOAc and filtered through SiO_2 (500 g), eluting with EtOAc. The filtrate was collected, concentrated, and purified by flash chromatography on a Biotage apparatus (75 M SiO_2, 17.5% v/v EtOAc in hexanes) to yield 4,7-dimethoxy-1*H*-pyrrolo[2,3-*c*]pyridine (9.80 g, 51%) as a white solid. HPLC retention time: 1.36 min (column B). ^{1}H NMR (DMSO-d_6): δ 3.87 (s, 3H), 3.96 (s, 3H), 6.45 (d, J = 2.6 Hz, 1H), 7.21 (s, 1H), 7.35 (dd, J = 2.6, 2.5 Hz, 1H), 11.74 (br s, 1H). ^{13}C NMR (DMSO-d_6): δ 52.4, 55.6, 99.0, 114.2, 121.1, 125.5, 126.6, 145.6, 145.8. MS *m*/*z* $(MH)^+$ calcd for $C_9H_{10}N_2O_2$: 179.08; found 179.05. HRMS *m*/*z* $(MH)^+$ calcd for $C_9H_{11}N_2O_2$: 179.0821; found 179.0811. Anal. Calcd for $C_9H_{10}N_2O_2\cdot0.2H_2O$: C, 59.46; H, 5.77; N, 15.41. Found: C, 59.48; H, 5.41; N, 15.63.

(4,7-Dimethoxy-1*H*-pyrrolo[2,3-*c*]pyridin-3-yl)oxoacetic Acid Ethyl Ester (12). Ethyl chlorooxoacetate (22.8 g, 167 mmol) was added to a stirred slurry of $AlCl_3$ (14.8 g, 111 mmol) in CH_2Cl_2 (320 mL). The solution was stirred for 1 h and then added dropwise over 1.5 h to a stirred slurry of 4,7-dimethoxy-1*H*-pyrrolo[2,3-*c*]pyridine (9.90 g, 56 mmol) and $AlCl_3$ (7.4 g, 56 mmol) in CH_2Cl_2 (265 mL). After 1 h, the red reaction mixture was poured over ice (1.1 kg) to afford a yellow solution which was extracted with CH_2Cl_2 (2 × 300 mL). The combined organic layers were concentrated to ∼100 mL, diluted with brine (200 mL), and concentrated to remove the remaining organic solvent. The residue was dissolved into EtOAc (800 mL), washed with H_2O (200 mL) and brine (200 mL), dried over $MgSO_4$, and concentrated. The combined aqueous layers were neutralized with $NaHCO_3$ (42 g) and extracted with EtOAc (3 × 600 mL) and the combined organic layers were dried over $MgSO_4$, concentrated, and combined with the previously obtained organic material to give a crude, yellow-brown oil (∼25 g). This material was purified by flash chromatography using a Biotage apparatus (75 M SiO_2, 50% v/v EtOAc in hexanes) to afford (4,7-dimethoxy-1*H*-pyrrolo[2,3-*c*]pyridin-3-yl)oxoacetic acid ethyl ester (13.5 g, 87%) as a yellow semisolid. LC purity: 98.0%. HPLC retention time: 1.28 min (column B). ^{1}H NMR (DMSO-d_6): δ 1.28 (t, J = 7.2 Hz, 3H), 3.83 (s, 3H), 3.99 (s, 3H), 4.32 (q, J = 7.2 Hz, 2H), 7.47 (s, 1H), 8.23 (s, 1H), 13.07 (br s, 1H). ^{13}C NMR (DMSO-d_6): δ 13.8, 52.9, 56.4, 61.3, 113.4, 118.8, 121.9, 122.5, 135.9, 145.5, 146.2,164.5. MS *m*/*z* $(MH)^+$ calcd for $C_{13}H_{15}N_2O_5$: 279.10; found 279.16.

Potassium (4,7-Dimethoxy-1*H*-pyrrolo[2,3-*c*]pyridin-3-yl)-oxoacetate (13). K_2CO_3 (28.58 g, 207 mmol) was added to a solution of (4,7-dimethoxy-1*H*-pyrrolo[2,3-*c*]pyridin-3-yl)oxo-acetic acid ethyl ester (28.74 g, 103 mmol) in a 1:1 mixture of MeOH/H_2O (500 mL), and the mixture was stirred for 6 h. The white precipitate was collected by filtration and washed with H_2O (10 mL) to afford **13** (18.0 g, 60%). LC purity: 95.3%. HPLC retention time: 0.69 min (column B). ^{1}H NMR (DMSO-d_6): δ 3.83 (s, 3H), 3.99 (s, 3H), 8.17 (s, 1H) 7.46 (s, 1H). ^{13}C NMR (DMSO-d_6): δ 52.8, 56.3, 113.6, 119.2, 121.9, 122.8, 135.8, 145.8, 146.2, 166.5, 183.0. MS m/z $(MH)^+$ of the corresponding acid of potassium 2-(4,7-dimethoxy-1*H*-pyrrolo[2,3-*c*]pyridin-3-yl)-2-oxoacetate calcd for $C_{11}H_{11}N_2O_5$: 251.07; found 251.09. HRMS m/z $(MH)^+$of the corresponding acid of potassium 2-(4,7-dimethoxy-1*H*-pyrrolo[2,3-*c*]pyridin-3-yl)-2-oxoacetate calcd for $C_{11}H_{11}N_2O_5$: 251.0668; found 251.0659.

1-(4-Benzoylpiperazin-1-yl)-2-(4,7-dimethoxy-1*H*-pyrrolo-[2,3-*c*]pyridin-3-yl)ethane-1,2-dione (BMS-488043, 4). ^{i}Pr$_2$Et-N (44.2 mL, 253 mmol) was added to a slurry of potassium 2-(4,7-dimethoxy-1*H*-pyrrolo[2,3-*c*]pyridin-3-yl)oxoacetate (26.1 g, 90.6 mmol) and benzoylpiperazine hydrochloride (30.8 g, 135.9 mmol) in DMF (800 mL). DEPBT (51.5 g, 172.1 mmol) in DMF (65 mL) was added dropwise over 15 min, and the mixture was stirred under nitrogen for 24 h before being concentrated. The residue was dissolved in EtOAc (1.6 L) and was washed with saturated aqueous $NaHCO_3$ (560 mL) and brine (700 mL). During each washing, the solid that formed between the layers was collected by filtration. The EtOAc layer was concentrated to ~200 mL and the precipitated solid collected and washed with EtOAc (2 × 100 mL). The solid material was combined to afford **4** (18. 0 g, 47%). HPLC retention time: 1.33 min (column B). Mp: 229.5−232 °C. ^{1}H NMR (DMSO-d_6): δ 3.63−3.34 (m, 8H), 3.83 (s, 3H), 4.00 (s, 3H), 7.40 (m, 6H), 8.15 (s, 1H), 13.0 (s, 1H). ^{13}C NMR (DMSO-d_6): δ 39.9, 45.5, 52.9, 56.8, 114.4, 119.2, 122.1, 122.2, 126.9, 128.4, 129.6, 135.3, 136.6, 145.7, 146.2, 166.5, 169.3, 185.5. MS m/z $(MH)^+$ calcd for $C_{22}H_{23}N_4O_5$: 423.17; found 423.19. Anal. Calcd for $C_{22}H_{21}N_4O_5 \cdot 0.2H_2O$: C, 62.17; H, 5.07; N, 13.18. Found: C, 61.92; H, 5.41; 13.01.

X-ray Crystal Structures of BMS-377806 (3) and BMS-488043 (4). Diffraction data were collected at room temperature using a Bruker SMART 2K CCD diffractometer equipped with graphite-monochromated Cu Kα radiation (λ = 1.540 56 Å). An empirical absorption correction utilized the SADABS routine (*SMART and SAINT-Plus Area Detector Control and Integration Software*; Bruker AXS: Madison, WI, 1998). The unit cell parameters were determined using the entire data set. The structures were solved by direct methods and refined by the full-matrix least-squares techniques, using the SHELXTL software package (Sheldrick, G. M. *SHELXTL. Structure Determination Programs*, version 5.10; Bruker AXS: Madison, WI, 1997). Non-hydrogen atoms were refined with anisotropic thermal displacement parameters. Hydrogen atoms involved in hydrogen bonding were located in the final difference Fourier maps, while the positions of the other hydrogen atoms were calculated from an idealized geometry with standard bond lengths and angles. They were assigned isotropic temperature factors and included in structure factor calculations with fixed parameters. Full crystallographic data have been deposited with the Cambridge Crystallographic Data Center (reference numbers CCDC 740492 (**3**), CCDC 717399 (**4**)). Copies of the data can be obtained free of charge via the Internet at http://www.ccdc.cam.ac.uk.

Antiviral Evaluation. Cells. 293T cells were obtained from the NIH AIDS Research and Reference Reagent Program, grown in DMEM with 10% heat inactivated FBS, 100 U/mL penicillin, and 100 μg/mL streptomycin and subcultured twice a week. The HeLa cell line expressing CD4, CCR5, and CXCR4 (HeLa 67 cells) was constructed at Bristol-Myers Squibb and maintained in the medium described above, supplemented with 400 μg/mL of zeocin, 100 μg/mL of hygromycin, and 200 μg/mL of Geneticin (G418). The last three antibiotics, used as selection markers, were omitted in the compound screen assay.

Pseudotype Reporter Virus. Pseudotype viruses HIV-1_{JRFL} LAI-Δenv-luc (JRFL-Luc) and HIV-1_{LAI} LAI-Δenv-luc (LAI-Luc) were prepared at Bristol-Myers Squibb by cotransfecting 293T cells with a plasmid containing proviral DNA of HIV-1 LAI-Δenv-luc (firefly luciferase in place of the envelope gene) and a plasmid expressing env (JRFL or LAI), driven by the HIV-LTR. The Lipofectamine Plus kit (Invitrogen) was used for transfection according to the package instructions. The pseudotype virus was harvested as cell supernatants on day 3 post-transfection and stored in 10 mL aliquots at −80 °C. The virus titer was determined in HeLa 67 cells using the assay protocol described below with a luciferase reporter gene assay (high sensitivity, Roche) as the end point. Virus input in the screen assays was normalized by the maximal luminescence signal.

Test Sample Preparation. Compounds were initially dissolved in 100% DMSO (30 mM stocks) and then 3-fold serially diluted in DMSO in 10 steps.

Drug Susceptibility Assay Using Pseudotype Reporter Viruses. Drug susceptibility was assessed in a single-cycle viral infection system.[54] The HIV LAI-Δenv-luc virus, pseudotyped with either the JRFL or LAI envelope, was used to infect HeLa 67 cells in the presence of serially diluted compounds. Cells were plated 1 day prior to infection at 10^5 cells per well in 100 μL of colorless medium. On the next day, duplicates of 2 μL of serially diluted compounds were per well into two replica plates. DMSO alone was used for the no-drug and no-virus controls. An amount of 100 μL per well of diluted virus stocks or 100 μL per well of medium (no-virus control) was added immediately after compound addition. Assay plates were incubated at 37 °C for 3 days. Virus yield was monitored by firefly luciferase activity 3 days after infection according to manufacturer's protocol (luciferase reporter gene assay, Roche).

Cytotoxicity Assay. Compound cytotoxicity was assayed in parallel for all experiments by exposing uninfected MT-2 cells to serially diluted compounds and measuring cell health after 3 days in an XTT assay,[55] according to the manufacturer's recommendations.

Data Analysis. The 50% effective concentration (EC_{50}) was calculated using the one ligand binding site model in XLFit for Microsoft Excel where percent inhibition = $1/[1+ (EC_{50}/\text{drug concn})^m]$ and m is a parameter that reflects the slope of the concentration−response curve. The CC_{50} values were calculated using the same equation.

Acknowledgment. The authors are grateful to Marie D'Andrea and Elizabeth Bitel (HRMS and CHN data), Dr. Xiaohua Stella Huang (NMR spectra), Dr. Richard A Dalterio, Gottfried Wenke, and Lirisa Zueva (pKa and log *D* measurements) for their assistance in obtaining analytical and physicochemical data. In addition, the preclinical candidate optimization organization at Bristol-Myers Squibb is acknowledged for in vitro and in vivo profiling of compounds **3** and **4**.

References

(1) Gallo, R. C.; Montagnier, L. The discovery of HIV as the cause of AIDS. *N. Engl. J. Med.* **2003**, *349*, 2283–2285.
(2) Pomerantz, R. J.; Horn, D. L. Twenty years of therapy for HIV-1 infection. *Nat. Med.* **2003**, *9*, 867–873.
(3) Barré-Sinoussi, F. The early years of HIV research: integrating clinical and basic research. *Nat. Med.* **2003**, *9*, 844–846.
(4) Merson, M. H. The HIV-AIDS pandemic at 25—the global response. *N. Engl. J. Med.* **2006**, *354*, 2414–2417.
(5) Richman, D. D.; Morton, S. C.; Wrin, T.; Hellmann, N.; Berry, S.; Shapiro, M. F.; Bozzette, S. A. The prevalence of antiretroviral drug resistance in the United States. *AIDS* **2004**, *18*, 1393–1401.

(6) Wainberg, M. A.; Brenner, B. G.; Turner, D. Changing patterns in the selection of viral mutations among patients receiving nucleoside and nucleotide drug combinations directed against human immunodeficiency virus type 1 reverse transcriptase. *Antimicrob. Agents Chemother*. **2005**, *49*, 1671–1678.

(7) Vella, S.; Palmisano, L. The global status of resistance to antiretroviral drugs. *Clin. Infect. Dis*. **2005**, *41* (Suppl. 4), S239–S246.

(8) Shafer, R. W.; Schapiro, J. M. Drug resistance and antiretroviral drug development. *J. Antimicrob. Chemother*. **2005**, *55*, 817–820.

(9) Little, S. J.; Holte, S.; Routy, J.-P.; Daar, E. S.; Markowitz, M.; Collier, A. C.; Koup, R. A.; Mellors, J. W.; Connick, E.; Conway, B.; Kilby, M.; Wang, L.; Whitcomb, J. M.; Hellman, N. S.; Richman, D. D. Antiretroviral drug resistance among patients recently infected with HIV. *N. Engl. J. Med*. **2002**, *347*, 385–394.

(10) Turner, D.; Wainberg, M. A. HIV transmission and primary drug resistance. *AIDS Rev*. **2006**, *8*, 17–23.

(11) De Clercq, E. Anti-HIV drugs: 25 compounds approved within 25 years after the discovery of HIV. *Int. J. Antimicrob. Agents* **2009**, *33*, 307–320.

(12) Doms, R. W.; Trono, D. The plasma membrane as a combat zone in the HIV battlefield. *Genes Dev*. **2000**, *14*, 2677–2688.

(13) Pierson, T. C.; Doms, R. W. HIV-1 entry inhibitors: new targets, novel therapies. *Immunol. Lett*. **2003**, *85*, 113–118.

(14) Kilby, J. M.; Eron, J. J. Novel therapies based on mechanisms of HIV-1 cell entry. *N. Engl. J. Med* **2003**, *348*, 2228–2238.

(15) Meanwell, N. A.; Kadow, J. F. Inhibitors of the entry of HIV into host cells. *Curr. Opin. Drug Discovery Dev*. **2003**, *6*, 451–461.

(16) Pierson, T. C.; Doms, R. W.; Pohlmann, S. Prospects of HIV-1 entry inhibitors as novel therapeutics. *Rev. Med. Virol*. **2004**, *14*, 255–270.

(17) Wang, H.-G. H.; Kadow, J. F.; Lin, P.-F. HIV gp120 envelope as a therapeutic target. *Drugs Future* **2005**, *30*, 359–367.

(18) Castagna, A.; Biswas, P.; Beretta, A.; Lazzarini, A. The appealing story of HIV entry inhibitors. *Drugs* **2005**, *65*, 879–904.

(19) Vermiere, K.; Schols, D. Anti-HIV agents targeting the interaction of gp120 with the cellular CD4 receptor. *Expert Opin. Invest. Drugs* **2005**, *14*, 1199–1212.

(20) Kadow, J. F.; Wang, H.-G. H.; Lin, P.-F. Small-molecule HIV-1 gp120 inhibitors to prevent HIV-1 entry: an emerging opportunity for drug development. *Curr. Opin. Invest. Drugs* **2006**, *7*, 721–726.

(21) Esté, J. A.; Telenti, A. HIV entry inhibitors. *Lancet* **2007**, *370*, 81–88.

(22) Schon, A.; Freire, E. Strategies for targeting the HIV-1 envelope glycoprotein gp120 in the development of new antivirals. *Future HIV Ther*. **2007**, *1*, 223–229.

(23) Strizki, J. Targeting HIV attachment and entry for therapy. *Adv. Pharmacol*. **2008**, *56*, 93–120.

(24) Qian, K.; Morris-Natschke, S. L.; Lee, K.-H. HIV entry inhibitors and their potential in HIV therapy. *Med. Res. Rev*. **2009**, *29*, 369–393.

(25) Wang, H.-G. H.; Williams, R. E.; Lin, P.-F. A novel class of HIV-1 inhibitors that targets the viral envelope and inhibits CD4 receptor binding. *Curr. Pharm. Des*. **2004**, *10*, 1785–1793.

(26) Wang, T.; Zhang, Z.; Wallace, O. B.; Deshpande, M.; Fang, H.; Yang, Z.; Zadjura, L .M.; Tweedie, D. L.; Huang, S.; Zhao, F.; Ranadive, S.; Robinson, B. S.; Gong, Y.-F.; Ricarrdi, K.; Spicer, T. P.; Deminie, C.; Rose, R.; Wang, H.-G. H.; Blair, W. S.; Shi, P.-Y.; Lin, P.-F.; Colonno, R. J.; Meanwell, N. A. Discovery of 4-benzoyl-1-[(4-methoxy-1*H*- pyrrolo[2,3-*b*]pyridin-3-yl)oxoacetyl]-2-(*R*)-methylpiperazine (BMS-378806): a novel HIV-1 attachment inhibitor that interferes with CD4-gp120 interactions. *J. Med. Chem*. **2003**, *46*, 4236–4239.

(27) Meanwell, N. A.; Wallace, O. B.; Fang, H.; Wang, H.; Deshpande, M.; Wang, T.; Yin, Z.; Zhang, Z.; Pearce, B. C.; James, J.; Yeung, K.-S.; Qiu, Z.; Wright, J. J. K.; Yang, Z.; Zadjura, L.; Tweedie, D. L.; Yeola, S.; Zhao, F.; Ranadive, S.; Robinson, B. A.; Gong, Y.-F.; Wang, H.-G. H.; Blair, W. S.; Shi, P.-Y.; Colonno, R. J.; Lin, P.-F. Inhibitors of HIV-1 attachment. Part 2: An initial survey of indole substitution patterns. *Bioorg. Med. Chem. Lett*. **2009**, *19*, 1977–1981.

(28) Lin, P.-F.; Blair, W. S.; Wang, T.; Spicer, T. P.; Guo, Q.; Zhou, N.; Gong, Y.-F.; Wang, H.-G. H.; Rose, R.; Yamanaka, G.; Robinson, B.; Li, C.-B.; Fridell, R.; Deminie, C.; Demers, G.; Yang, Z.; Zadjura, L.; Meanwell, N. A.; Colonno, R. J. A small molecule HIV-1 inhibitor that targets the HIV-1 envelope and inhibits CD4 receptor binding. *Proc. Natl. Acad. Sci. U.S.A*. **2003**, *100*, 11013–11018.

(29) Guo, Q.; Ho, H.-T.; Dicker, I.; Fan, L.; Zhou, N.; Friborg, J.; Wang, T.; McAuliffe, B. V.; Wang, H.-G. H.; Rose, R. E.; Fang, H.; Scarnati, H. T.; Langley, D. R.; Meanwell, N. A.; Abraham, R.; Colonno, R. J.; Lin, P.-F. Biochemical and genetic characterizations of a novel human immunodeficiency virus type 1 inhibitor that blocks gp120-CD4 interactions. *J. Virol*. **2003**, *77*, 10528–10536.

(30) Ho, H.-T.; Fan, L.; Nowicka-Sans, B.; McAuliffe, B.; Li, C.-B.; Yamanaka, G.; Zhou, N.; Fang, H.; Dicker, I.; Dalterio, R.; Gong, Y.-F.; Wang, T.; Yin, Z.; Ueda, Y.; Matiskella, J.; Kadow, J. F.; Clapham, P.; Robinson, J.; Colonno, R. J.; Lin, P.-F. Envelope conformational changes induced by human immunodeficiency virus type 1 attachment inhibitors prevent CD4 binding and downstream entry events. *J. Virol*. **2006**, *80*, 4017–4025.

(31) Si, Z.; Madani, N.; Cox, J. M.; Chruma, J. J.; Klein, J. C.; Schon, A.; Phan, N.; Wang, W.; Biorn, A. C.; Cocklin, S.; Chaiken, I.; Freire, E.; Smith, A. B.; Sodroski, J. G. Small-molecule inhibitors of HIV-1 entry block receptor-induced conformational changes in the viral envelope glycoproteins. *Proc. Natl. Acad. Sci U.S.A*. **2004**, *101*, 5036–5041.

(32) Madani, N.; Perdigoto, A. L.; Srinivasan, K.; Cox, J. M.; Chruma, J. J.; LaLonde, J.; Head, M.; Smith, A. B., III; Sodroski, J. G. Localized changes in the gp120 envelope glycoprotein confer resistance to human immunodeficiency virus entry inhibitors BMS-806 and #155. *J. Virol*. **2004**, *78*, 3742–3752.

(33) Hanna, G.; Lalezari, J.; Hellinger, J.; Wohl, D.; Masterson, T.; Fiske, W.; Kadow, J. F.; Lin, P.-F.; Giordano, M.; Colonno, R. J.; Grasela, D. Antiviral Activity, Safety, and Tolerability of a Novel, Oral Small-Molecule HIV-1 Attachment Inhibitor, BMS-488043, in HIV-1-Infected Subjects. Presented at the 11th Conference on Retroviruses Opportunistic Infections, San Francisco, CA, February 8−11, **2004**; Abstract 141.

(34) Catalan, J.; Mo, O.; Pérez, P.; Yañez, M. Influence of the tautomeric forms of azaindoles on their basicity in solution. *J. Mol. Struct*. **1984**, *107*, 263–368.

(35) Hlavica, P. Functional interaction of nitrogenous organic bases with cytochrome P450: a critical assessment and update of substrate features and predicted key active-site elements steering the access, binding, and orientation of amines. *Biochim. Biophys. Acta* **2006**, *1764*, 645–670.

(36) Rendic, S. Summary of information on human CYP enzymes: human P450 metabolism data. *Drug Metab. Rev*. **2002**, *34*, 83–448.

(37) Tehan, B. G.; Lloyd, E. J.; Wong, M. G.; Pitt, W. R.; Gancia, E.; Manallack, D. T. Estimation of pK_a using semiempirical molecular orbital methods. Part 2: application to amines, anilines and various nitrogen containing heterocyclic compounds. *Quant. Struct.−Act. Relat*. **2002**, *21*, 473–485.

(38) Perrin, D. D. *Dissociation Constants of Organic Bases in Aqueous Solution*; Butterworths: London, 1965; Supplement to Pure Appl. Chem.

(39) Zhang, Z.; Yang, Z.; Meanwell, N. A.; Kadow, J. F.; Wang, T. A general method for the preparation of 4- and 6-azaindoles. *J. Org. Chem*. **2002**, *67*, 2345–2347.

(40) Van de Poel, H.; Guillaumet, G.; Viaud-Massuard, M.-C. Synthesis of melatonin analogues derived from furo-[2,3-*b*]- and [2,3-*c*]-pyridines by use of a palladium-copper catalyst system. *Heterocycles* **2002**, *57*, 55–71.

(41) Yamato, T.; Hideshima, C.; Tashiro, M. A convenient preparation and inclusion behavior of 1,3,5-tris-(hydroxyphenyl)benzenes. *Chem. Express* **1990**, *5*, 845–848.

(42) Zhang, Z.; Yang, Z.; Wong, H.; Zhu, J.; Meanwell, N. A.; Kadow, J. F.; Wang, T. An effective procedure for the acylation of azaindoles at C-3. *J. Org. Chem*. **2002**, *67*, 6226–6227.

(43) Li, H.; Jiang, X.; Ye, Y.-h.; Fan, C.; Romoff, T.; Goodman, M. 3-(Diethoxyphosphoryloxy)-1,2,3-benzotriazin-4(3*H*)-one (DEPBT): a new coupling reagent with remarkable resistance to racemization. *Org. Lett*. **1999**, *1*, 91–93.

(44) Tobyn, M.; Brown, J.; Dennis, A. B.; Fakes, M.; Gao, Q.; Gamble, J.; Khimyak, Y. Z.; McGeorge, G.; Patel, C.; Sinclair, W.; Timmins, P. Amorphous drug−PVP dispersions: application of theoretical, thermal and spectroscopic analytical techniques to the study of a molecule with intermolecular bonds in both the crystalline and pure amorphous state. *J. Pharm. Sci*. **2009**, *98*, 3456–3468.

(45) Brameld, K. A.; Kuhn, B.; Reuter, D. C.; Stahl, M. Small molecule conformational preferences derived from crystal structure data. A medicinal chemistry focused analysis. *J. Chem. Inf. Model*. **2008**, *48*, 1–24.

(46) Johnson, F. Allylic strain in six-membered rings. *Chem. Rev*. **1968**, *68*, 375–413.

(47) Chevallier, F.; Beaudet, I.; Grognec, E. L.; Toupet, L.; Quintard, J.-P. Allylstannation of *N*-acyliminium intermediates: a possible method for the stereocontrolled synthesis of polyhydroxypiperidines. *Tetrahedron Lett*. **2004**, *45*, 761–764.

(48) Wang, T.; Kadow, J. F.; Zhang, Z.; Yin, Z.; Gao, Q.; Wu, D.; DiGiugno Parker, D.; Yang, Z.; Zadjura, L.; Robinson, B. A.; Gong, Y.-F.; Blair, W. S.; Shi, P.-Y.; Yamanaka, G.; Lin, P.-F.; Meanwell, N. A. Inhibitors of HIV-1 attachment. Part 4: A study of

the effect of piperazine substitution patterns on antiviral potency in the context of indole-based derivatives. *Bioorg. Med. Chem. Lett.* **2009**, *19*, 5140–5145.

(49) Lin, P.-F; Ho, H.-T.; Gong, Y.-F.; Dicker, I.; Zhou, N.; Fan, L.; McAuliffe, B.; Kimmel, B.; Nowicka-Sans, B.; Wang, T.; Kadow, J. F.; Yamanaka, G.; Yin, Z.; Yang, Z.; Zadjura, L.; Meanwell, N. A.; Colonno, R. J. Characterization of a Small Molecule HIV-1 Attachment Inhibitor BMS-488043: Virology, Resistance and Mechanism of Action. Presented at the 11th Conference on Retroviruses Opportunistic Infections, San Francisco, CA, February 8−11, **2004**; Abstract 534.

(50) Yang, Z.; Zadjura, L.; Marino, A.; D'Arienzo, C.; Malinowski, J.; Gesenberg, C.; Lin, P.-F.; Colonno, R. J.; Wang, T.; Kadow, J. F.; Meanwell, N. A.; Hansel, S. Utilization of in vitro caco-2 permeability and microsomal half-life screens in discovering BMS-488043, a novel HIV-1 attachment inhibitor with improved pharmacokinetic properties. Unpublished results.

(51) Hanna, G.; Yan, J.-H.; Fiske, W.; Masterson, T.; Zhang, D.; Grasela, D. Safety, Tolerability, and Pharmacokinetics of a Novel Small-Molecule of HIV-1 Attachment Inhibitor, BMS-488043, after Single and Multiple Oral Doses in Healthy Subjects. Presented at the 11th Conference on Retroviruses Opportunistic Infections, San Francisco, CA, February 8−11, **2004**; Abstract 535.

(52) Fakes, M. G.; Vakkalagadda, B. J.; Qian, F.; Desikan, S.; Gandhi, R. B.; Lai, C.; Hsieh, A.; Franchini, M. K.; Toale, H.; Brown, J. Enhancement of oral bioavailability of an HIV-1 attachment inhibitor by nanosizing and amorphous dispersion approaches. *Int. J. Pharm.* **2009**, *370*, 167–174.

(53) Ueda, Y.; Connolly, T. P.; Kadow, J. F.; Meanwell, N. A.; Wang, T.; Chen, C.-P. H.; Yeung, K.-S.; Zhang, Z.; Leahy, D. K.; Pack, S. K.; Soundararajan, N.; Sirard, P.; Levesque, K.; Thoraval, D. Prodrugs Based on Bicyclic Nitrogen-Containing Heterocyclic Antiviral Agents Having Substituted Piperazine or Piperidine Rings. U.S. Pat. Appl. Publ. US 2005209246 A1, **2005**.

(54) Johnson, V. A.; Byington, R. T. Infectivity Assay (Virus Yield Assay). *Techniques in HIV Research*; New York, 1990.

(55) Cory, A. H.; Owen, T. C.; Barltrop, J. A.; Cory, J. G. Use of an aqueous soluble tetrazolium/formazan assay for cell growth assays in culture. *Cancer Commun.* **1991**, *3*, 207–212.

(56) Yang, Z.; Zadjura, L. M.; D'Arienzo, C.; Marino, A.; Santone, K.; Klunk, L.; Greene, D.; Lin, P.-F.; Colonno, R. J.; Wang, T.; Meanwell, N. A.; Hansel, S. Preclinical pharmacokinetics of a novel HIV-1 attachment inhibitor BMS-378806 and prediction of its human pharmacokinetics. *Biopharm. Drug Dispos.* **2005**, *26*, 387–402.